Science of the Total Environment 954 (2024) 176119

Contents lists available at ScienceDirect

Science of the Total Environment

journal homepage: www.elsevier.com/locate/scitotenv

Microbial community respiration kinetics and their dynamics in coastal seawater

Henry L.S. Cheung [a,b,1], Rachel L. Simister [c], Christelle Not [a,b], Sean A. Crowe [a,b,c,*]

[a] Department of Earth Sciences, The University of Hong Kong, Pok Fu Lam Road, Hong Kong Special Administrative Region
[b] The Swire Institute of Marine Sciences, The University of Hong Kong, Pok Fu Lam Road, Hong Kong Special Administrative Region
[c] Departments of Microbiology and Immunology, and Earth, Ocean, and Atmospheric Sciences, University of British Columbia, 2350 Health Sciences Mall, Vancouver, British Columbia V6T19 1Z3, Canada

HIGHLIGHTS

- Maximum respiration rates and affinity for oxygen in coastal seawater varied seasonally.
- Coastal communities exhibit relatively high affinities for oxygen.
- Respiration proceeded to oxygen concentrations <100 nmol L^{-1}.
- Temperature, nutrient content, and productivity influence respiration kinetics.
- Respiration kinetics varied with community composition.

GRAPHICAL ABSTRACT

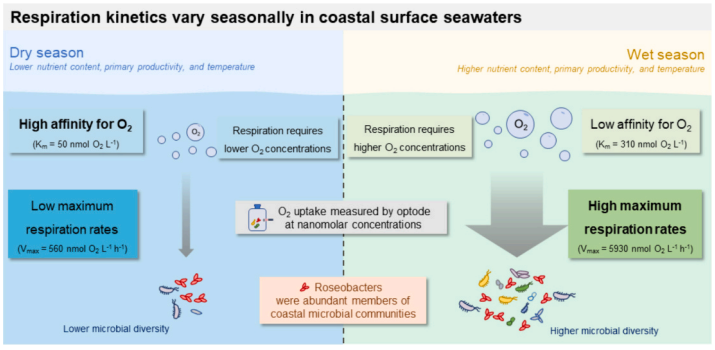

ARTICLE INFO

Editor: Jay Gan

Keywords:
Ocean deoxygenation
Respiration kinetics
Microbial community
Optodes
Coastal seawater
Anthropogenic influences

ABSTRACT

Oxygen (O_2) concentrations in coastal seawater have been declining for decades and models predict continued deoxygenation into the future. As O_2 declines, metabolic energy use is progressively channelled from higher trophic levels into microbial community respiration, which in turn influences coastal ecology and biogeochemistry. Despite its critical role in deoxygenation and ecosystem functioning, the kinetics of microbial respiration at low O_2 concentrations in coastal seawater remain uncertain and are mostly modeled based on parameters derived from laboratory cultures and a limited number of environmental observations. To explore microbial responses to declining O_2, we measured respiration kinetics in coastal microbial communities in Hong Kong over the course of an entire year. We found the mean maximum respiration rate (V_{max}) ranged between 560 ± 280 and 5930 ± 800 nmol O_2 L^{-1} h^{-1}, with apparent half-saturation constants (K_m) for O_2 uptake of between 50 ± 40 and 310 ± 260 nmol O_2 L^{-1}. These kinetic parameters vary seasonally in association with shifts in microbial community composition that were linked to nutrient availability, temperature, and biological productivity. In general, coastal communities in Hong Kong exhibited low affinities for O_2, yet communities in the dry season had higher affinities, which may play a key role in shaping the relationship between community size,

* Corresponding author at: Departments of Microbiology and Immunology, and Earth, Ocean, and Atmospheric Sciences, University of British Columbia, 2350 Health Sciences Mall, Vancouver, British Columbia V6T19 1Z3, Canada.
E-mail address: sean.crowe@ubc.ca (S.A. Crowe).
[1] Present address: Department of Marine Sciences, University of Gothenburg, Gothenburg, Sweden.

https://doi.org/10.1016/j.scitotenv.2024.176119
Received 27 May 2024; Received in revised form 30 August 2024; Accepted 5 September 2024
Available online 21 September 2024

biomass, and O_2 consumption rates through respiration. Overall, parameters derived from these experiments can be employed in models to predict the expansion of deoxygenated waters and associated effects on coastal ecology and biogeochemistry.

1. Introduction

Marine habitats are increasingly characterized by O_2 concentrations below 63 μmol L^{-1}, the conventional threshold for hypoxia, with many progressing towards anoxia (Breitburg et al., 2018; Diaz and Rosenberg, 2008). Such low O_2 conditions develop where biological O_2 consumption via aerobic respiration persistently exceeds the rate of O_2 supply through physical transport and oxygenic photosynthesis (Calvert and Price, 1971; Fuenzalida et al., 2009; Stramma et al., 2010; Wyrtki, 1962). Oxygen loss, or deoxygenation, in both the open ocean and in coastal waters is accelerating due both to increased global temperatures and anthropogenic nutrient inputs (Breitburg et al., 2018; Schmidtko et al., 2017). Coastal ecosystems that receive municipal effluents are also increasingly reporting eutrophication and an associated decline in O_2 through time due to elevated microbial respiration (Breitburg et al., 2018). Low O_2 concentrations can strongly impact marine ecological and biogeochemical processes (Robinson et al., 2002). For example, decreasing O_2 concentrations alter heterotrophic respiration, ultimately leading to engagement of anaerobic pathways that, in turn, influence ecosystem energetics and carbon flow (Wright et al., 2012). Oxygen availability, furthermore, affects biomass remineralization and related sinks and sources for many bioessential elements, including nitrogen, phosphorus, and iron (Breitburg et al., 2018; Keeling et al., 2010; Wright et al., 2012).

To effectively manage coastal ecosystems, reliable predictions of deoxygenation and its impacts are critical. However, many existing numerical models tend to underestimate the rate of O_2 decline (Stramma et al., 2012). Poor constraints on relevant biological responses and feedbacks underpin key uncertainties in existing model predictions (Oschlies et al., 2018; Stramma et al., 2012). For example, progressive deoxygenation increasingly channels respiration through microorganisms (Robinson, 2019; Wright et al., 2012). Empirical information on microbial respiration as a function of O_2 concentrations is thus required to more accurately predict the effects of O_2 availability on rates of deoxygenation, and hence to improve model outputs. The predictive rate equations used to describe rates of microbial respiration as a function of substrate concentrations and often take the form of Michaelis-Menten models (Canfield et al., 2005). Kinetic parameters in these models - maximum respiration rates (V_{max}) and apparent half-saturation constants (K_m) – can be used to describe aerobic respiration rates as a function of O_2 concentrations and are the basis for many biogeochemical models (Canfield et al., 2019).

Microbial respiration kinetics have mainly been explored in model bacterial strains (Gong et al., 2016; Stolper et al., 2010; Trojan et al., 2021), with some studies extending to marine microbial communities (Garcia-Robledo et al., 2016; Gong et al., 2016; Revsbech and Glud, 2009; Tiano et al., 2014a). Advancement in optical O_2 sensing technologies are providing new opportunities for precise rate measurements across a range of O_2 concentrations (Bittig et al., 2018; Medina-Sánchez et al., 2017; Vikström et al., 2019). Application of optical O_2 sensors, or optodes, allows direct, quantitative, and high-resolution analyses of microbial respiration through incubation experiments (Garcia-Robledo et al., 2016; Gong et al., 2016; Holtappels et al., 2014) enabling systematic exploration of microbial community respiration kinetics via time-series experimentation.

The specific objective of this study is to determine rates of microbial respiration as a function of O_2 concentrations and to develop the corresponding predictive rate equations—we thus measured respiration rates in coastal seawater microbial communities from Hong Kong. We conducted a year-long time-series experiment, which allowed us to track dynamics in respiration rates and ecophysiology across seasons. Collectively, our experiments reveal considerable seasonal variability in respiration kinetics that need to be considered in models of coastal ocean deoxygenation and its corresponding ecological and biogeochemical impacts.

2. Materials and methods

2.1. Study site and sampling

Seawater samples were collected from sheltered coastal waters in Aberdeen Harbour (22°14.91′N, 114°9.36′E) in Hong Kong, where anthropogenic activities cause high organic carbon loading (Leong and Tanner, 1999). Surface waters were sampled over the course of a year in both the wet (May to October) and dry seasons (November to April) of 2020 and 2021, in order to determine possible variation in respiration kinetic properties associated with dynamics in water quality and microbial community compositions. For each sampling event, seawater was pre-filtered through a 100 μm mesh screen, to remove large organisms and macro-debris, and collected into 10 L cubitainers. Samples were transported back to the lab on ice within an hour of collection. Once the samples arrived in the lab, a peristaltic pump was used to pre-filter the seawater through a 2.7 μm GF/D pre-filter (Whatman) to select for free-living microbial community members in the filtrate and to remove larger grazing organisms and minimize their interference on O_2 uptake measurements. While we do not capture respiration from particle-associated microbiota, our results should capture respiration by the core free-living communities also targeted in many microbial community profiling studies using the same filtration strategy (Torres-Beltrán et al., 2019). To collect microbial biomass for community DNA extraction, 2 L of pre-filtered water was further filtered onto 0.22 μm Sterivex filters (Millipore). Microbial biomass for community composition analyses after the incubation experiment in April 2021 was collected by filtering water directly from the serum bottles onto 0.22 μm Durapore filters (Millipore). After each filtration, 1.8 mL of sucrose lysis buffer (EDTA: 40 mM; Tris: 50 mM; Sucrose: 0.75 M) was added to the filters. All filters were stored at −80 °C until DNA extraction and purification.

2.2. Incubation experiments

A suite of incubations was conducted in glass-serum bottles to measure O_2 consumption as a function of time to determine microbial O_2 uptake rates. A trace O_2 sensor spot with detection limit of 60 nmol O_2 L^{-1} (TROXSP5, Pyroscience) was fixed to the inner wall of a 250 mL-glass serum bottles (Kimble) with silicone glue. The silicone was allowed to cure 1-day at room temperature before the experiment. Before each incubation experiment, a two-point calibration was performed for each sensor spot. The zero concentration calibration point was set in a 0.3 M sodium dithionite solution, and the upper calibration point was set with air-saturated water. Incubation bottles with calibrated sensor spots were then sterilized by autoclave. To start the incubation, ~240 mL of GF/D pre-filtered seawater sample was transferred to autoclaved incubation bottles containing a sterilized glass-coated magnetic stir bar (Sigma). Pre-filtered seawater in each bottle was then purged for around 15 min with N_2 gas to reduce dissolved O_2 concentrations to approximately 5000–10,000 nmol O_2 L^{-1} in an effort to minimize the duration of incubation needed to draw oxygen down and the "bottle effects" associated with longer-term incubations (Tiano et al., 2014b). After purging, bottles were then closed with sterile, 1.5 cm thick, blue butyl rubber

stoppers to prevent introduction of O_2 to the bottle from the atmosphere.

Experiments began immediately after the elimination of the headspace, which was done by displacing the headspace gas with N_2-purged pre-filtered seawater to a final volume of 250 mL. A 1 mL air-tight syringe with a 1.25-in. long 22G hypodermic needle was then inserted through the stopper for pressure compensation. The bottles were then placed in a thermostated water bath at 24 ± 1 °C, which is the annual average temperature in Aberdeen Harbour (Environmental Protection Department, 2019), to minimize the influence of temperature variations on respiration rates and the optode O_2 measurements. A stir plate (IKA Labortechnick) was placed underneath each bottle to ensure the water was well-mixed. A temperature sensor (TDIP15, Pyroscience) was placed into the water bath, which allows automatic real-time temperature compensation. The fluorescent signals from the optodes were read via optical fibres (SPFIB-BARE-CL2, Pyroscience) positioned outside the bottles. Oxygen concentrations were measured every second and recorded using the software Pyro Workbench V1.2.0.1359.

2.3. Microbial community DNA extraction

Microbial community genomic DNA was extracted from Sterivex filters as previously described (Hawley et al., 2017; Zaikova et al., 2010), with modification. Briefly, after thawing on ice, 100 μL lysozyme (0.125 mg mL^{-1}; Sigma) and 20 μL of RNAse A (1 μL mL^{-1}; Thermo Fisher) were added and incubated at 37 °C for 1 h in a hybridization oven. After this incubation, 100 μL Proteinase K (Sigma) and 100 μL 20 % SDS were added to the filters, which were then incubated at 55 °C for 2 h. Lysate was transferred into a 15 mL centrifuge tube by a sterile syringe and followed with an additional rinse of the filter with 1 mL of lysis buffer. Microbial genomic DNA was extracted from the lysates using the phenol:chloroform extraction method. Extracted genomic DNA was purified by washing three times with TE buffer (pH 8.0) using a 10 KD 15 mL Amicon filter cartridge (Millipore) and concentrated to a final volume of between 100 and 300 μL. Genomic DNA from Durapore filters was extracted as follows: filter segments were transferred to a 15 mL centrifuge tube followed by addition of 1.8 mL lysis buffer and 100 μL 20 % SDS. Filters were shaken vigorously and then subjected to phenol:chloroform extraction and processed as described above for Sterivex filters. Total DNA concentrations were determined by the PicoGreen assay (Life Technologies) and DNA quality assessed by visualization on 0.8 % agarose gel (2 h at 80 V).

2.4. SSU rRNA gene amplification and sequencing

DNA for amplicon sequencing was prepared based on Apprill et al. (2015) and Caporaso et al. (2011). To prepare the amplicon library, primers 515F (5′-GTG YCA GCM GCC GCG GTA A-3′) (Parada et al., 2016) and 806R (5′-GGA CTA CNV GGG TWT CTA AT-3′) (Apprill et al., 2015) were used to amplify bacterial and archaeal SSU rRNA gene fragments from the extracted genomic DNA. An Agilent Bioanalyzer was used to determine approximate library fragment size and to verify library integrity, by the High Sensitivity DS DNA assay. KAPA Library Quantification Kit for Illumina was used to determine the DNA concentration in library pools. Library pool was diluted to 4 nmol L^{-1} and denatured into single strands using fresh 0.2 M NaOH. With an additional PhiX spike-in of 5–20 %, the library was loaded at 8 pM. Sequencing was conducted on the Ilumina MiSeq platform.

2.5. 16S rRNA sequence data analysis

Sequences of the 16S rRNA gene were processed through Mothur (Schloss et al., 2009). Briefly, sequences with ambiguous characters, had homopolymers longer than 8 bp, and did not align to a reference alignment of the correct sequencing region were removed. A pre-clustering algorithm was used to denoise sequences within the sample (Schloss et al., 2011). A SILVA alignment was used to identify and align unique sequences (http://www.mothur.org/wiki/Silva_reference_alignment). Chimeric sequences were removed by UCHIME (Edgar et al., 2011). Sequences were then clustered into 97 % OTUs by OptiClust (Westcott and Schloss, 2017). OTUs were classified with reference to the SILVA taxonomy database (release 138, http://www.mothur.org/wiki/Silva_reference_files). OTUs with one 16S rRNA sequence read were removed. All data was visualized in R and GraphPad Prism version 9.2.0 (San Diego, CA). For alpha and beta diversity measures, all samples were subsampled to the lowest coverage depth ($n = 29{,}256$) and calculated in Mothur. Hierarchical clustering was performed using the hclust and dist functions in RStudio, and a principal coordinates analysis (PCoA) was used to compare bacterial and archaeal community structures across all samples, using the vegdist and pcoa functions in RStudio.

2.6. Nutrients and chlorophyll a measurement

Samples for nutrient concentration measurements were immediately filtered, transferred to the lab on ice, and stored at −20 °C for later analysis. Samples for nitrate (NO_3^-) and nitrite (NO_2^-), ammonium (NH_4^+) and inorganic phosphate (PO_4^-) determinations were thawed immediately prior to analysis and measured with spectrophotometric methods: the Griess assay, the indophenol blue method, and the modified Murphy and Riley procedure, respectively (Grasshoff et al., 2009). Total NO_x (NO_3^- and NO_2^-) was measured by reducing NO_3^- to NO_2^- with vanadium (García-Robledo et al., 2014), and subtracting NO_2^- from the total NO_x to obtain NO_3^- concentrations. The absorbances were all measured on a MultiSkan Go Microplate Spectrophotometer (Thermo Fisher).

Seawater samples for chlorophyll *a* concentration measurements were first transported to the lab in amber HDPE bottles on ice. Biomass in the seawater samples was collected onto GF-75 filters, which were extracted for 24 h with 90 % buffered acetone solution (90 parts acetone and 10 parts saturated magnesium carbonate solution) at −20 °C, and the extracted chlorophyll *a* measured on a NanoDrop One^C Microvolume UV–Vis Spectrophotometer (Thermo Fisher). The concentration of chlorophyll *a* was calculated according to the Lorenzen method (Lorenzen, 1967).

2.7. Calculation of rates and rate constants

Oxygen uptake rates were calculated from linear regression of O_2 concentration data. Data collected in the first 10 min to 3 h of the experiments (before linear O_2 depletion was observed) were discarded as this period allowed microorganisms to acclimate to stable conditions after sampling and handling (Johnson, 1967; Tiano et al., 2014b). Kinetic parameters were determined based on changes in O_2 concentration as a function of time. The raw data were first fit and smoothed with a 6th order polynomial spline. Oxygen concentrations recorded below 2000 nmol O_2 L^{-1} were used to determine O_2 uptake rates, calculated as the slopes of linear regressions over oxygen consumption intervals at different O_2 concentrations: from 2000 to 1000 nmol O_2 L^{-1}, slopes were calculated for every 200 nmol O_2 L^{-1}; from 1000 to 100 nmol O_2 L^{-1} for every 100 nmol O_2 L^{-1}; and from 100 to 60 nmol O_2 L^{-1} for every 10 nmol O_2 L^{-1}. A non-linear regression was then used to fit a Michaelis-Menten-type enzyme kinetic model (MM) to the resulting rate data as a function of O_2 concentrations using GraphPad Prism version 9.2.0 (San Diego, CA):

$$R = V_{max} \times \frac{[O_2]}{K_m + [O_2]} \quad (1)$$

Here R represents the O_2 uptake rate, V_{max} is the maximum respiration rate, which is at the highest O_2 concentration ($[O_2]$), and K_m is the O_2 concentration at half the maximum rate.

Biomass-specific V_{max} was determined by dividing the volume-specific V_{max} by total biomass. Total biomass was calculated according to Khachikyan et al. (Khachikyan et al., 2019). Briefly, cell volumes were calculated by assuming that cell width equals to cell height:

$$V = \pi r^2 \times h + \frac{4}{3}\pi r^3 \quad (2)$$

Here V is the cell volume in cubic micrometres, r is the radius of a cell, and $h = L - 2r$, where L is the length of the cell. Based-on the typical morphology and the high abundance of Proteobacteria HIMB11 and Cyromorphaceae spp. (Bowman, 2014; Durham et al., 2014) across sampling events, cell volumes were calculated by assuming the size of cells were generally 2 μm long and radius of 0.5 μm. The dry mass in femtograms (m_{dry}) was then calculated as:

$$m_{dry} = 322 \times V^{0.43} \quad (3)$$

Total biomass in each incubation was then calculated from total cell number, which was assumed to be 16×10^5 cells mL^{-1}, according to previously reported average numbers from adjacent southern waters that range from 7 to 100×10^5 cells mL^{-1} (Yuan et al., 2010). Specific affinities for O_2 were calculated by dividing biomass specific V_{max} by the K_m value (Button, 1998). Cell specific V_{max} was determined by dividing the volume-specific V_{max} by total cell number.

The temperature dependence of microbial respiration was further assessed through the Arrhenius relationship based on cell specific respiration rates (Raven and Geider, 1988):

$$lnR = a - b\left(\frac{1}{kT}\right) \quad (4)$$

where R is the cell specific V_{max}, k is Boltzmann's constant of $8.62\ 10^{-5}$ eV K^{-1}, T is the in situ water temperature in K, and b is the negative slope in the Arrhenius plot that corresponds to the activation energy (E_a, eV). A temperature sensitivity coefficient (Q_{10}) was further derived as $Q_{10} = \exp.(10E_a/RT^2)$, where R is the gas constant of 8.314 mol^{-1} K^{-1} and T is the mean water temperature in K. Value of E_a was converted to J mol^{-1} by conversion factor of 96,486.9 J eV^{-1} mol^{-1}.

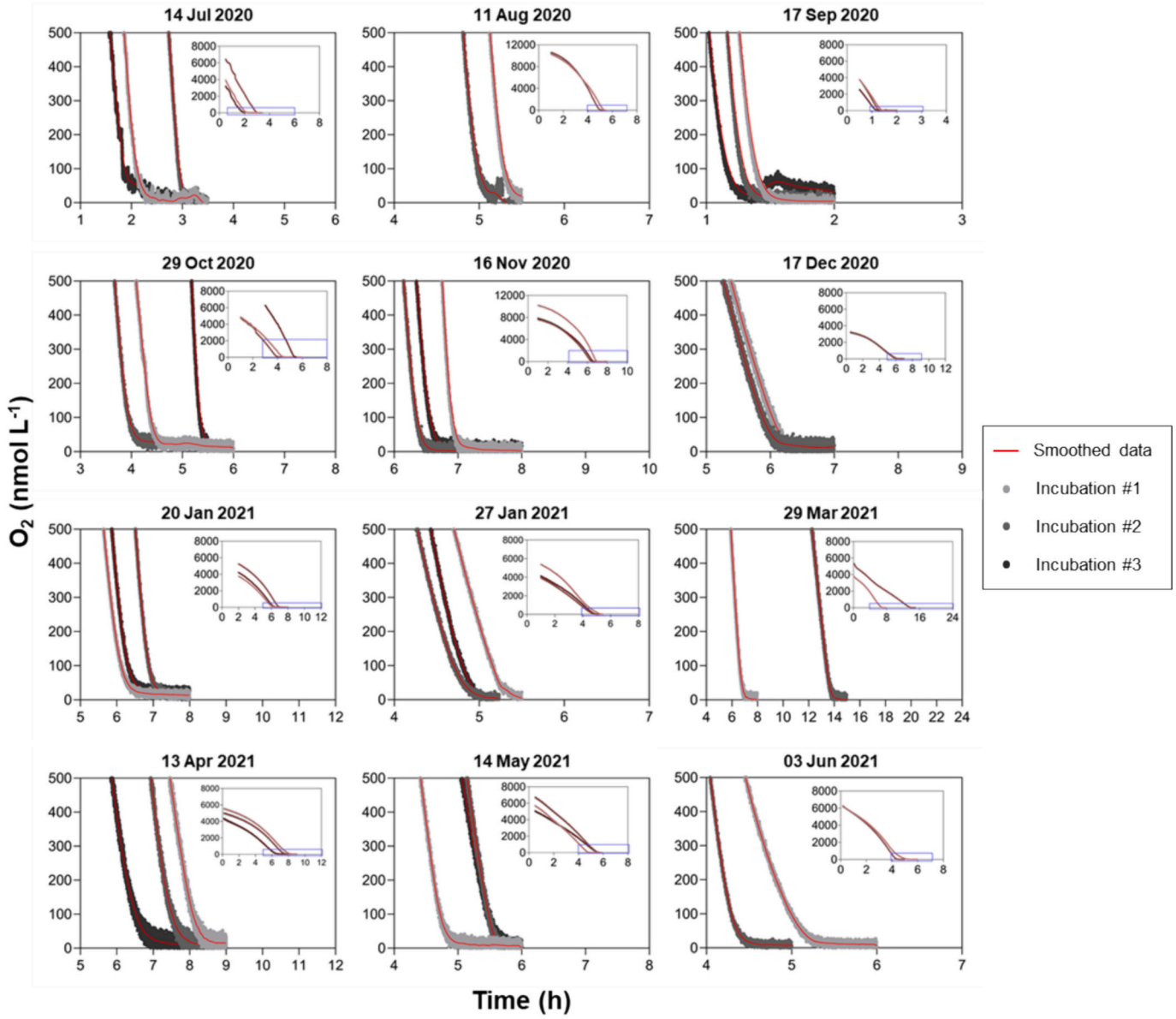

Fig. 1. Oxygen depletion as a function of time in surface seawaters from Aberdeen Harbour, Hong Kong. Plots show O_2 concentrations as a function of time below 500 nmol O_2 L^{-1} with 2–3 replicates for a given sampling. Oxygen concentrations were smoothed (red line) and used to determine O_2 uptake rates. Colours denote replicates of incubations (n = 2–3). The inset delineates all data collected and blue frame delineates data below 500 nmol O_2 L^{-1}.

3. Results and discussion

3.1. Microbial community respiration in Hong Kong coastal water

In all incubations, O_2 concentrations declined monotonically as the result of microbial respiration (Fig. 1). Oxygen uptake rates exhibited pronounced reduction when O_2 concentrations in the incubation reached ~100 nmol L^{-1}—well above the sensor detection limit of 60 nmol O_2 L^{-1}. Community O_2 uptake rates were estimated by fitting smoothed O_2 depletion curves into Michaelis-Menten model as a function of O_2 concentrations, with coefficients of determination (R^2) ranging from 0.90 ± 0.01 to 0.99 ± 0.00 (Fig. 2). We found mean apparent half-saturation constants (K_m) for O_2 between 65 ± 19 and 310 ± 260 nmol O_2 L^{-1}. Based on the average total cell number in surface waters adjacent to our study site (Yuan et al., 2010), we estimated specific affinity for O_2 in the communities of between 12,100 ± 1400–36,100 ± 3900 L g^{-1} cells h^{-1}, with a mean value of 23,900 ± 8100 L g^{-1} cells h^{-1} (Table 1). As total cell number could range from 7 to 100 × 10^5 cells mL^{-1} in surface seawater seasonally (Yuan et al., 2010), mean specific affinity could range from 3800 ± 1300 to 54,700 ± 18,500 L g^{-1} cells h^{-1}. Our estimated mean value was lower than that derived by global average cell number in surface seawater (6.9 × 10^5 cells mL^{-1}; Gram et al., 2010) of 55,500 ± 18,700 L g^{-1} cells h^{-1}, which likely due to the higher cell number in sub-tropical Hong Kong waters. More detailed investigations on specific affinity for O_2 should be conducted in the future. Furthermore, we found a linear relationship between K_m and V_{max} ($p < 0.05$, Fig. 3a) as expected based on typical enzyme kinetic properties, where enzymes with high substrate affinity (high K_m) bind substrates strongly and therefore tend to turn over substrate more slowly (low V_{max}), and vice versa (Seibert and Tracy, 2021; Wallenstein et al., 2011; Wang et al., 1992). This, therefore, supports the expected dependence of microbial respiration rates on affinities for O_2 in natural settings.

Respiration kinetics observed for microbial communities in Hong Kong seawaters compare well with previously investigated temperate coastal waters (Tiano et al., 2014b). The K_m values derived from our experiments are similar to the range reported for Danish coastal waters of 93 ± 25 to 310 ± 61 nmol O_2 L^{-1} (Tiano et al., 2014b), regardless of the higher seawater temperature in Hong Kong (18–28 °C) than in Denmark (15–21 °C). Measurements from all incubations in Hong Kong

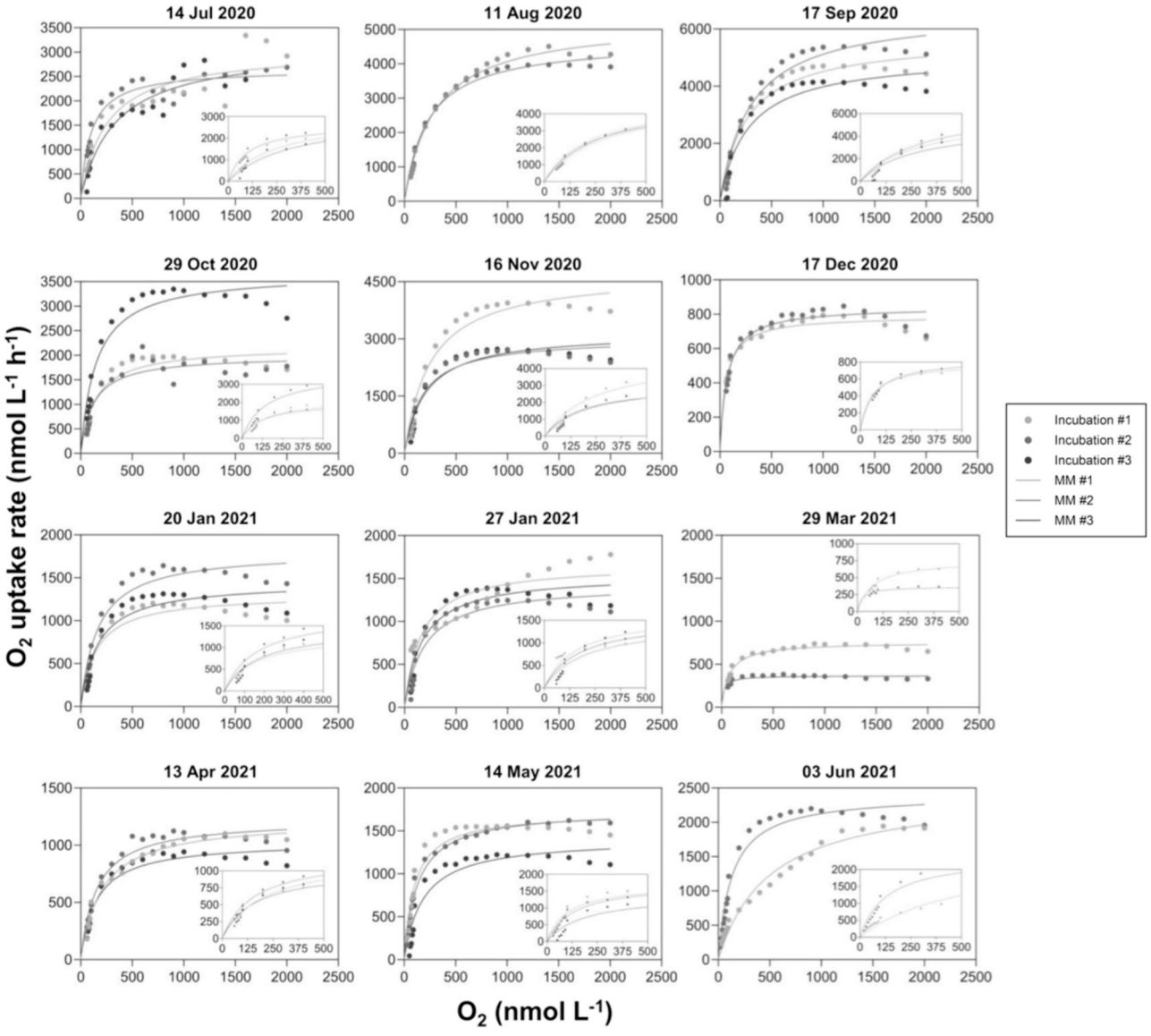

Fig. 2. Oxygen uptake rates as a function of oxygen concentration in surface seawaters from Aberdeen Harbour, Hong Kong. Oxygen uptake rates plotted as a function of oxygen concentrations. Rates were fit to a Michaelis-Menten type enzyme kinetic model (MM). The inset delineates data collected below 500 nmol O_2 L^{-1}.

Table 1
Respiration kinetic parameters for Hong Kong coastal marine microbial communities and corresponding environmental metadata for context.

Date	V_{max} (nmol L^{-1} h^{-1})	K_m (nmol L^{-1})	n	R^2	Cell specific V_{max} (fmol O_2 L^{-1} h^{-1})	Specific affinity (L g^{-1} cells h^{-1})	Temp. (°C)	NH_4^+ (μmol L^{-1})	NO_3^- (μmol L^{-1})	NO_2^- (μmol L^{-1})	PO_4^{3-} (μmol L^{-1})	Chlorophyll *a* (μg L^{-1})
14-Jul-2020	2980 ± 270	250 ± 130	3	0.92 ± 0.02	1.9 ± 0.2	28,000 ± 15,900	28.2	1.0 ± 0.1	10.2 ± 0.1	1.4 ± 0	0.2 ± 0.1	24.4 ± 0.8
11-Aug-2020	5010 ± 420	270 ± 50	2	0.99 ± 0.00	3.1 ± 0.3	34,700 ± 3100	28.1	2.3 ± 0.4	8.3 ± 0.4	2.0 ± 0.0	0.2 ± 0.1	7.1 ± 0.2
17-Sep-2020	5930 ± 800	310 ± 20	3	0.94 ± 0.03	3.7 ± 0.5	36,100 ± 3900	27.3	7.0 ± 0.1	7.8 ± 0.3	1.8 ± 0.0	1.2 ± 0.3	3.9 ± 0.5
29-Oct-2020	2670 ± 930	160 ± 10	3	0.91 ± 0.03	1.7 ± 0.6	31,100 ± 9200	28.3	1.2 ± 0.1	2.6 ± 0.1	1.9 ± 0.0	0.6 ± 0.0	3.9 ± 0.5
16-Nov-2020	3720 ± 950	230 ± 40	3	0.93 ± 0.01	2.3 ± 0.6	29,700 ± 3300	24.2	1.9 ± 0.4	5.5 ± 0.2	0.8 ± 0.0	0.8 ± 0.1	1.0 ± 0.1
17-Dec-2020	820 ± 50	60 ± 20	2	0.94 ± 0.00	0.5 ± 0.0	24,600 ± 6000	20.1	1.5 ± 0.1	7.8 ± 0.4	0.9 ± 0.1	0.7 ± 0.1	0.7 ± 0.1
20-Jan-2021	1550 ± 260	190 ± 10	3	0.92 ± 0.02	1.0 ± 0.2	15,700 ± 2300	18.0	1.0 ± 0.5	6.5 ± 0.2	0.7 ± 0.0	0.6 ± 0.1	1.2 ± 0.1
27-Jan-2021	1540 ± 100	170 ± 30	3	0.90 ± 0.01	1.0 ± 0.1	17,000 ± 3800	18.2	2.2 ± 1.1	4.4 ± 0.3	0.3 ± 0.1	0.5 ± 0.2	1.2 ± 0.3
29-Mar-2021	560 ± 280	50 ± 40	3	0.91 ± 0.08	0.3 ± 0.1	15,300 ± 11,400	21.9	1.7 ± 0.1	1.1 ± 0.2	n.d.	0.3 ± 0.1	1.6 ± 0.4
13-Apr-2021	1170 ± 110	180 ± 20	3	0.96 ± 0.02	0.7 ± 0.1	12,100 ± 1400	23.7	2.1 ± 0.2	1.6 ± 0.1	n.d.	0.2 ± 0.0	0.8 ± 0.2
14-May-2021	1620 ± 180	140 ± 40	3	0.94 ± 0.04	1.0 ± 0.1	23,800 ± 8900	27.0	0.8 ± 0.1	15.1 ± 0.4	1.9 ± 0.0	n.d.	14.3 ± 1.4
3-Jun-2021	2430 ± 30	310 ± 260	2	0.97 ± 0.01	1.3 ± 0.4	19,400 ± 13,400	27.4	3.3 ± 0.1	13.2 ± 0.3	4.5 ± 0.0	0.7 ± 0.0	2.2 ± 0.1

Mean ± standard deviation of maximum respiration rates (V_{max}), apparent half-saturation constant (K_m), number of replicates (n), cell specific V_{max}, specific affinity for O_2, in situ water temperature (Temp.), concentration of chlorophyll *a*, and concentrations of water nutrients (μmol L^{-1}): ammonium (NH_4^+), nitrate (NO_3^-), nitrite (NO_2^-), and phosphate (PO_4^{3-}). Average R^2 values assesses the goodness of fit of the Michaelis-Menten model. In situ water temperature were obtained from the monitoring station adjacent to Aberdeen Harbour, operated by the Hong Kong Environmental Protection Department (Environmental Protection Department, 2020, 2021). n.d. = not detected.

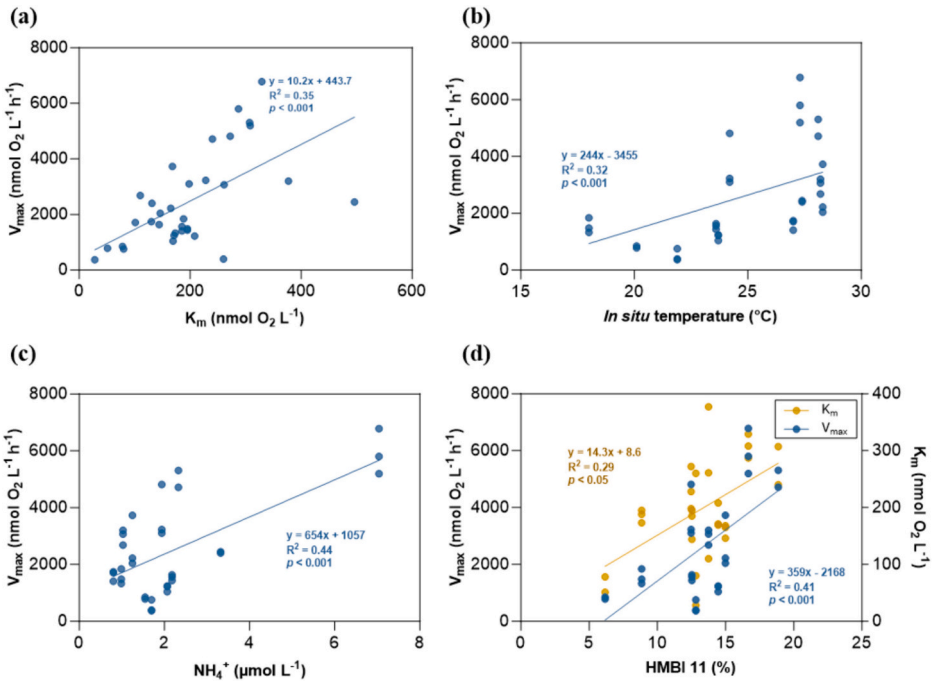

Fig. 3. Plots of kinetic parameters as a function of other variables. (a) Correlation between maximum respiration rate (V_{max}) and ammonium (NH_4^+) concentrations (b) Correlation between V_{max} and in situ water temperature. (c) Correlation between V_{max} and apparent half-saturation constants (K_m) (d) Correlation between V_{max}, K_m, and relative abundance of HIMB 11 in the communities.

yielded mean K_m values of 200 ± 90 nmol O_2 L^{-1}, which is typical, 200 ± 2 nmol O_2 L^{-1}, of low-affinity aerobic terminal oxidases (Rice and Hempfling, 1978). Metagenomic analyses of coastal microbial communities in well-oxygenated waters from the Gulf of Maine and a Norwegian fjord indeed find a prevalence of low-affinity aerobic terminal oxidases (Morris and Schmidt, 2013). Low-affinity terminal oxidases (cytochrome *c* oxidases) also dominate the terminal oxidase pool in the Eastern Pacific Ocean, where most were assigned to the

Proteobacterial phylum (Kalvelage et al., 2015).

Proteobacteria dominated microbial community compositions in Danish coastal surface waters (Traving et al., 2016). This observation is similar to our observation that Proteobacteria make up to a mean value 64.0 ± 7.1 % in Hong Kong coastal waters (Fig. 4a). Community K_m values in Hong Kong coastal waters are similar to low-affinity terminal oxidases. Previous studies reported the expression of similar K_m values for diverse marine and other Proteobacteria (30–200 nmol O_2 L^{-1}) (Chu et al., 2022; Gong et al., 2016; Stolper et al., 2010). Microbial respiration rates often vary across ecosystems in response to environmental conditions such as temperature, while similar K_m values measured in subtropical and temperate coastal communities imply that affinity for O_2 may not respond strongly to temperature differences. Most of the taxa present in both communities process low-affinity oxidases (Morris and Schmidt, 2013). By extension affinity for O_2 in coastal microbial communities may be comparable, possibly even over large geographic distances. Such similarity could be linked to the dominance of bacterial species with low-affinity oxidases in marine waters in general. Nevertheless, measurements of respiration kinetics coupled with community profiling in coastal waters are limited and thus further investigation is needed to properly establish global extensibility.

Seawater microbial communities in Hong Kong exhibit relatively low-affinity for O_2 throughout the year, but higher-affinities can be observed episodically. In general, higher affinities for O_2 were observed in the dry season ($p = 0.06$, Supplementary Table 1). Respiration with higher affinity for O_2, was pronounced in December and March, which exhibited low community K_m values of 60 ± 20 and 50 ± 40 nmol O_2 L^{-1}, respectively. The higher affinities for O_2 could be linked to the potential activity of microbial community members capable of aerobic respiration through high-affinity oxidases. For example, *Candidatus* Actinomarina of the Actinobacteria process high-affinity genes in their genomes (López-Pérez et al., 2020), and comprise up to 8.8 and 11.8 % of the Hong Kong seawater community in December 2020 and March 2021, respectively (Fig. 4b). If such organisms indeed have higher affinities for O_2 we suggest that they may emerge as key contributors to aerobic respiration in the low O_2 waters that develop in the dry season in response to deoxygenation.

Despite similarities in affinities for O_2, maximum respiration rates (V_{max}) in surface seawater microbial communities varied seasonally (Fig. 5a). Mean V_{max} values of 3440 ± 1660 and 1560 ± 1130 nmol O_2 L^{-1} h^{-1} were measured in the wet and dry seasons, respectively, and these differences are statistically significant ($p < 0.05$) among seasons

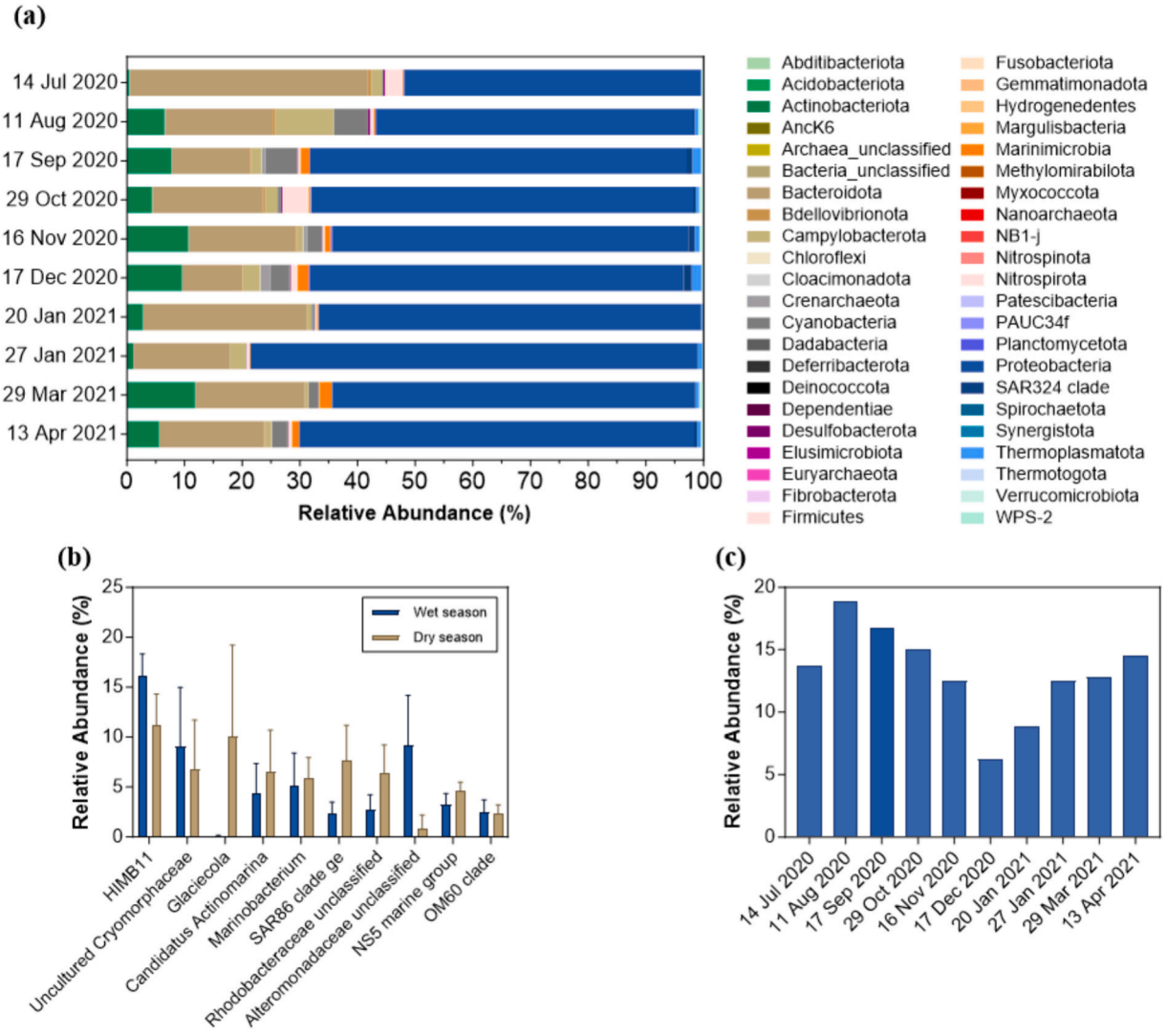

Fig. 4. Microbial community compositions and taxonomy in seawater from Aberdeen Harbour, Hong Kong. (a) Relative abundance of OTUs classified at phylum level in the samples. The relative abundance of reads for each OTU was calculated as a percentage of the total reads for each sample. (b) Mean abundance of the top 10 most abundant OTUs classified at genus level in the samples from each season. Blue and yellow bars indicate mean abundance of the genus in wet and dry season, respectively. Error bars indicate standard errors. (c) Relative abundance of Roseobacter sp. HIMB 11 in seawater.

(Supplementary Table 1). Similar seasonal patterns were observed in previous studies on community respiration in Hong Kong's surface water, with a higher mean community respiration rate in July (729 ± 155 nmol O_2 L^{-1} h^{-1}) and lower rates in November (316 ± 131 nmol O_2 L^{-1} h^{-1}) (Yuan et al., 2010). The lowest rate of 560 ± 280 nmol O_2 L^{-1} h^{-1} (March 2021) was found in spring at water temperature of 22 °C, which was lower, yet comparable, to coastal Danish waters of 761 ± 76 nmol O_2 L^{-1} h^{-1} in the summer at 21 °C (Tiano et al., 2014b). Higher V_{max} can be explained by the significantly higher water temperature in summer that is up to 28 °C ($p < 0.01$, Supplementary Table 1), given that water temperature and V_{max} for coastal water in Hong Kong were significantly correlated ($p < 0.001$, Fig. 3b). pH and salinity, which can also affect rates of microbial respiration (Dupont et al., 2014; James et al., 2017), were relatively uniform throughout the year (7.8 ± 0.1 and 30.8 ± 0.8, respectively) (Environmental Protection Department, 2019). No significant correlation between these parameters and respiration kinetics was observed. This implies that, likely because of their limited variability, these variables are not strong controls on respiration rates in the Hong Kong waters studied. Instead, water temperature appears to be a stronger predictor of seasonal variation in coastal respiration rates in Hong Kong.

Variation in coastal microbial respiration has a strong dependence on water temperature, and this can generally be described by the Arrhenius relationship (Robinson, 2019). We derived a temperature sensitivity coefficient (Q_{10}) of 3.15 and an activation energy (E_a) of 0.87 eV. This Q_{10} value for coastal microbial communities in Hong Kong is higher than that determined for mesopelagic respiration in seawater with temperature that ranged between 9 and 15 °C, implying that community respiration in Hong Kong coastal surface water is more sensitive to temperature dynamics. This is consistent with the observation that the rates we measured are generally higher than those from other published locations given that the majority of reported measurements are from temperate regions (Robinson and Williams, 2005), where water temperature is generally lower (Lønborg et al., 2021). Overall, our results imply that rates of community respiration can vary across ecosystems, which is likely a combined function of temperature, productivity, and organic carbon loading differences between systems (Wikner et al., 2023).

Perhaps counterintuitively, respiration was characterized by relatively low affinity during the wet season—a time in which hypoxic conditions (<63 μmol O_2 L^{-1}) commonly develop in Hong Kong waters (Chen et al., 2022; Qian et al., 2018). This contrasts with expectations for higher affinity for O_2 at low O_2 concentrations (Bueno et al., 2011; Morris and Schmidt, 2013). Such observations may reflect a prevalence of low-affinity oxidases at this time of year in Hong Kong waters, which would be consistent with a dominance of low-affinity oxidases previously observed even at nanomolar O_2 concentrations, (Trojan et al., 2021). Microbial communities may display low affinity respiration as their preferred energy conservation strategy under high nutrient conditions in the summer, even under hypoxic conditions of 12.5–50.0 μmol O_2 L^{-1} in Hong Kong waters (Chen et al., 2022; Qian et al., 2018). Note that even these depressed O_2 concentrations are much higher than the K_m value of both high- and low-affinity oxidase (3–8 and 200 nmol O_2 L^{-1}, respectively) (Morris and Schmidt, 2013), the latter of which are presumably best-suited to support respiration under hypoxic conditions. On the other hand, the higher affinities observed in the dry season may reflect low nutrient availability, aligning with studies reporting lower K_m values for marine bacterial respiration under nutrient limitation (Gong et al., 2016). It may thus be that nutrient availability is a strong lever on community respiration, even in light of O_2 concentrations as low as 12.5 μmol L^{-1} in Hong Kong during the wet season. This should be explored in more detail in the future.

3.2. *Nutrient loading and productivity control coastal community respiration*

Variation in the rates of community respiration are often the result of changes to nutrient loading and corresponding dynamics in primary

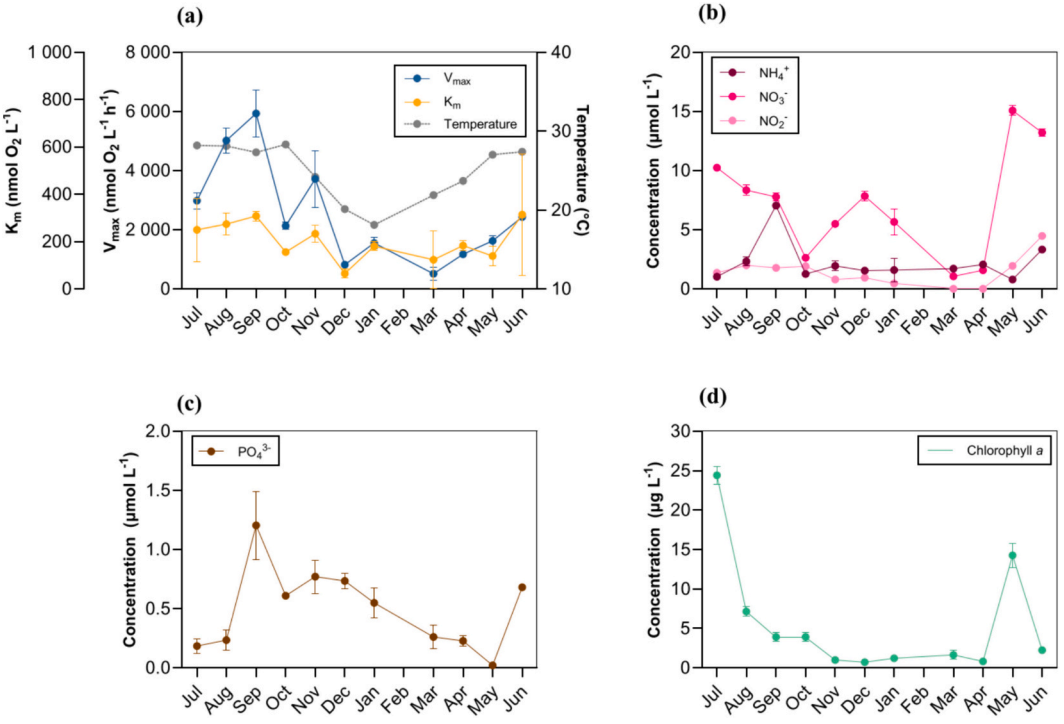

Fig. 5. Respiration kinetics and environmental parameters over the year in Aberdeen, Hong Kong. (a) Values of maximum respiration rates (V_{max}), apparent half-saturation constants (K_m), and surface water temperature. (b) concentrations of ammonium (NH_4^+), nitrate (NO_3^-), and nitrite (NO_2^-) (c) concentration of phosphate (PO_4^{3-}) (d) concentrations of chlorophyll *a*. Error bars indicated standard deviations. Note that mean values in January were derived from measurements in 20th and 27th January 2021.

productivity (del Giorgio and Duarte, 2002). In our analyses of Hong Kong coastal waters, higher nitrogen loading was observed in wet seasons which also had higher respiration rates. Significant differences were found in NO_3^- and NO_2^- ($p < 0.05$, Supplementary Table 1), and higher concentrations of both species were observed in the wet season (Fig. 5b). This observation was consistent with enhanced nutrient inputs, including NO_3^-, in wet seasons as the result of elevated atmospheric deposition, run-off from rainfall and rivers, and groundwater discharge (Archana et al., 2018; Yau et al., 2020).

Elevated microbial community respiration rates have been attributed to anthropogenic impacts in coastal waters around Hong Kong (Yuan et al., 2010). Nitrogen loading promotes eutrophication, which is associated with enhanced heterotrophic respiration, and this can eventually lead to deoxygenation (Breitburg et al., 2018; Rabalais et al., 2002; Robinson, 2019). Nitrification driven by anthropogenic NH_4^+ is coupled to autotrophic O_2 uptake, which can also account for a substantial fraction of total O_2 uptake (Hsiao et al., 2014; Ward, 2008). Furthermore, we observed a positive correlation between V_{max} and NH_4^+ ($p < 0.001$, Fig. 3c). Elevated NH_4^+ concentrations presumably promotes nitrification, which in turn enhances NO_3^- availabilities for phytoplankton (Han et al., 2017), and presumably subsequent primary productivity.

We also observe that wet-season waters exhibit a statistically higher concentrations of chlorophyll *a* ($p < 0.05$, Fig. 5d). The concentration of chlorophyll *a* reflects the abundance of photosynthetic organisms and hence also primary productivity (Gong et al., 2000), or the net balance between primary production and respiration, which generally correlates positively to gross rates of microbial respiration in coastal waters (Iriarte et al., 1997; Jensen et al., 1990; Robinson, 2019). Our observations of both elevated nitrogen and chlorophyll *a* that co-occur with high respiration rates support the idea that nutrient driven enhancements to productivity lead to elevated rates of O_2 respiration in Hong Kong coastal waters.

3.3. Variability in respiration kinetics with community composition

Respiration kinetics may reflect microbial community composition and structure as kinetic descriptions of aerobic respiration are intrinsically linked to the affinities for O_2 in members of microbial communities. Microbial communities in Hong Kong coastal water cluster primarily according to season (Fig. 6a). Results of PCoA illustrate greater similarity between waters of the same season, with members of the Bdellovibrionota and Actinobacteriota driving significant differences in community composition between the wet and dry seasons (Fig. 6b). Similarity in respiration kinetics may arise due to similar microbial community compositions with correspondingly similar metabolic potential and O_2 demand. There are, however, very few prior measurements of respiration in coastal microbial communities with parallel information on microbial community composition and structure with which to compare. Nonetheless, prior studies in Hong Kong coastal waters reveal community compositions similar to those determined here, with Proteobacteria and Bacteroidetes dominating (Zhang et al., 2007). The similarly in community composition across studies, is consistent with previous measurements of community respiration, which were also similar to our observations (Yuan et al., 2010). More nuanced variability in respiration kinetics observed between seasons may, nevertheless, reflect the more granular differences in microbial compositions observed at lower taxonomic ranks.

Respiration kinetics may also relate to species richness in microbial communities. Microbial communities in the wet season exhibited significantly higher species richness than in the dry season with correspondingly higher respiration rates. The estimated species richness (Chao1) was variable across the year, and these results are summarized in Supplementary Table 2, with values that ranged from 501 to 1600 OTUs. The average species richness in wet season was 1100 ± 300 OTUs, while in dry season was 700 ± 100 OTUs. Significant differences were found between seasons with $p < 0.05$ (Supplementary Table 1). This observation is consistent with previous observations from freshwater systems, which suggested microbial diversity positively correlated with microbial respiration (Delgado-Baquerizo et al., 2016). Likewise, previous studies from oxygen minimum zones (OMZs) implied that microbial diversity facilitates adaptation to low O_2 conditions, with possible links to the presence of high-affinity and low-affinity terminal oxidases (Bertagnolli and Stewart, 2018; Murillo et al., 2014). High microbial diversity was also reported as a key factor in sediment microbial community resilience in the face of deoxygenation (Sinkko et al., 2019). Our results suggest that microbial community diversity is linked to elevated aerobic respiration and possibly to overall rates of microbial

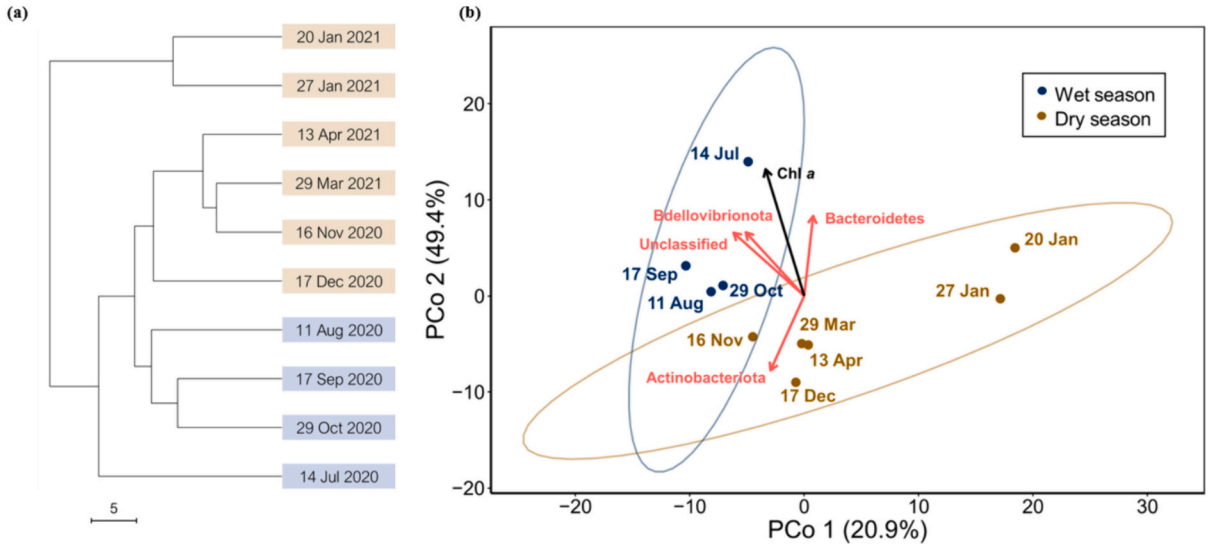

Fig. 6. Seasonal variations of microbial community composition in seawater from Aberdeen between July 2020 to April 2021. (a) Dendrogram clustering represents the Euclidean dissimilarity of community profiles. The scale bar of the dendrogram represents the dissimilarity level (%) between communities. Communities in wet and dry season were coloured in blue and yellow, respectively (b) Comparison of community composition between seasons by principal coordinate analysis (PCoA) biplot based on Euclidean dissimilarity method. Red and black arrows represent the significant correlation ($p < 0.05$) of microbial phyla and environmental parameters (i.e., chlorophyll *a* concentration, Chl a) with PCoA axes, respectively. Ellipses represent communities between seasons with significant differences (Euclidean distance; $p < 0.05$; PERMANOVA).

community activity, with seasonal effects on both.

3.4. Roseobacter dominated coastal community respiration

Dominance of Roseobacter species across sampling events is in line with the idea that Roseobacter populations play an outsized role in respiration and carbon cycling in coastal waters. In all samples investigated, the top 10 most abundant genera comprised mainly members from Proteobacteria, with a Roseobacter sp. HIMB11 as the most abundant genus (Fig. 4b), representing between 6.2 and 18.9 % of the seawater community throughout the time period of our observations (Fig. 4c). In addition, relative abundance of the Roseobacter sp. HIMB11 in the communities was positively correlated with both V_{max} and K_m values (Fig. 3d).

As one of the most populous bacterial lineages (up to 20 %) in ocean surface waters, Roseobacters are considered key players in coastal marine biogeochemical cycles (Luo and Moran, 2014). Notably, Roesobacters are known to play an outsized role in aerobic respiration, and they can contribute up to 37 % of the total O_2 uptake in coastal waters even when they only represent 1.2–2.5 % of the total microbial community (Munson-McGee et al., 2022). It is also worth noting the similarity of the respiration kinetics determined for pure Roseobacter cultures and the Roseobacters dominated Hong Kong seawater communities, with mean K_m values of 300 ± 250 and 200 ± 90 nmol O_2 L^{-1}, respectively (Chu et al., 2022). This implies that kinetics obtained from pure cultures of dominant species can reflect those derived from natural communities. High relative abundances of Roseobacters in the Hong Kong seawater communities and their positive correlations with respiration kinetics, further suggests that the kinetic properties of coastal communities and their responses to deoxygenation may be disproportionately influenced by Roseobacter respiration. Also, respiration kinetics determined for Hong Kong microbial communities may be more broadly extensible to similar marine systems around the globe, to the extent that Roseobacters and other key community members exhibit similar physiology across systems.

The abundance of the Proteobacterial SAR11 cluster, which is one of the most abundant groups of microorganisms in the oceans, was exceptionally low in Hong Kong coastal waters. SAR11 populations dominate surface microbial communities in most the oligotrophic oceans (Brown et al., 2012; Carlson et al., 2009; Jing et al., 2013; Tsementzi et al., 2016), while low abundances have also been reported from other coastal regions (Cottrell and Kirchman, 2000). The low abundance of SAR11 population across all seasons sampled implies a limited role for SAR11 respiration in Hong Kong waters and other coastal areas, where meso- to copiotrophic organisms, such as Roseobacters, are likely more important.

3.5. Microbial composition changes after deoxygenation

After the incubation experiment conducted in April 2021, the community composition from the bottles was analysed and compared with the in situ composition. Changes in community composition were observed after incubation at low O_2 concentrations (Fig. 7). The most apparent change is the enrichment of *Glaciecola* sp., which increased from around 6.0 % to an average of 46.0 ± 6.0 %, after up to 9 h of incubation. Arcobacteraceae sp. increased from 0.5 % to an average of

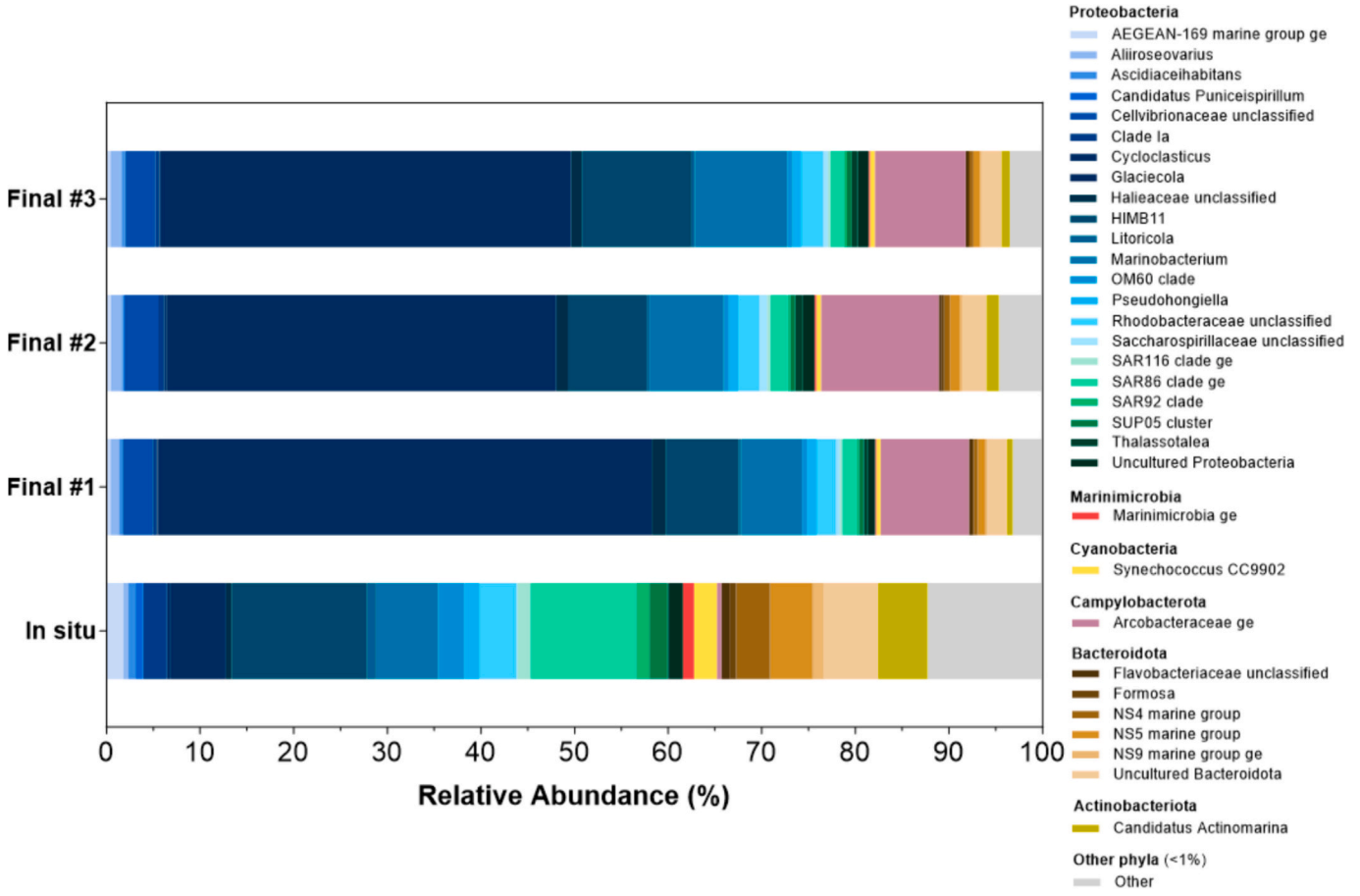

Fig. 7. Microbial community compositions based on 16S rRNA gene sequencing in three replicate bottles after the incubation experiment. In situ microbial community compositions (In situ), as well as microbial community in three incubation bottles after 9 h incubation (Final #1, #2, and #3) in April 2021 were analysed. The relative abundance of reads for each genus was calculated as a percentage of the total reads for each sample.

11.0 ± 2.0 %. In contrast, some species diminished in abundance after the incubation. For example, SAR86 sp. dropped from 11.3 % down to 1.6 ± 0.2 %. Additionally, the abundance of the NS5 marine group and *Candidatus* Actinomarina also decreased from 4.6 % to 0.9 ± 0.1 and 5.0 to 0.9 ± 0.4 %, respectively. These observations imply that low O_2 conditions may lead to potential loss of some bacterial species, and therefore proportionally increase those tolerant of low O_2 levels.

Changes in community composition after incubation suggest that the experimentally induced low O_2 concentrations reshape microbial community compositions. Some microorganisms, for example *Glaciecola* sp. and Arcobacteraceae sp., were enriched after the incubation (Fig. 7). The strictly aerobic chemoheterotroph *Glaciecola* sp. (Baik et al., 2006; Bowman et al., 1998) was conspicuously enriched under reduced O_2 concentrations in our incubations. Although there is little existing physiological information, *Glaciecola* sp. was identified in the OMZ off the coast Chile (Stevens and Ulloa, 2008), which suggests that *Glaciecola* sp. may be adapted to low O_2 conditions. Also, Arcobacteraceae sp. are conspicuous members of low O_2 marine environments, including model systems like Saanich Inlet (Michiels et al., 2019), as well as open ocean OMZs, more broadly (Wright et al., 2012). Many Arcobacteraceae sp. are facultative aerobes with capacity to grow anaerobically using substrates like sulphide and iron (Martinez-Malaxetxebarria et al., 2012; Miller et al., 2007; Roalkvam et al., 2015; van der Stel and Wösten, 2019). While unintentional, the observed shifts in microbial community composition provide insight into changes expected during deoxygenation, which might thus be tracked by monitoring the distribution of organisms like the Arcobacteraceae sp.

On the other hand, there was a reduction in the relative abundance of other species following incubation, indicating a lack of tolerance for low O_2 by some community members. For example, the apparent reduction in Proteobacteria SAR86. SAR86 appears to be an obligate aerobic heterotroph (Dupont et al., 2012), which seems to have struggled under the low-O_2 conditions in our incubations. Additionally, the abundances of the NS5 marine group and *Candidatus* Actinomarina also decreased, despite evidence suggesting these organisms process high-affinity terminal oxidases (López-Pérez et al., 2020; Ngugi and Stingl, 2018). Our results thus imply strong potential shifts in microbial community composition in response to deoxygenation.

4. Conclusions

We determined microbial community respiration kinetics as a function of O_2 concentrations using incubation experiments with optode sensors and natural coastal microbial communities across seasons in Aberdeen, Hong Kong. In general, microbial communities in Hong Kong coastal waters exhibited low affinity for O_2 yet exhibit potential to adapt to lower concentrations with higher-affinity O_2 uptake. Seasonal variability in microbial respiration rates can be linked to nutrient supply and productivity and clear clustering in microbial community compositions between wet and dry seasons corelate with changes in respiration kinetics. Roseobacter sp. HIMB 11, was identified as the dominant bacterial species across all seasons, and this highlights the key role of Roseobacters in coastal respiration. Overall, our study revealed seasonal variation in coastal microbial respiration linked to dynamics in temperature, nutrient availability and primary productivity, as well as microbial community composition. Kinetic parameters derived from this study can be employed in models of biogeochemical cycling and deoxygenation in Hong Kong coastal waters and may be further extensible to global coastal areas, more generally. Our results underscore the importance of considering seasonal variability not only in respiration rates, but also in the underlying kinetic parameters, in models attempting to forecast seawater O_2 concentrations in coastal marine environments.

Supplementary data to this article can be found online at https://doi.org/10.1016/j.scitotenv.2024.176119.

CRediT authorship contribution statement

Henry L.S. Cheung: Writing – original draft, Methodology, Investigation, Formal analysis, Data curation, Conceptualization. **Rachel L. Simister:** Writing – review & editing, Investigation, Formal analysis. **Christelle Not:** Writing – review & editing, Supervision, Funding acquisition. **Sean A. Crowe:** Writing – review & editing, Supervision, Methodology, Investigation, Funding acquisition, Conceptualization.

Declaration of competing interest

The authors declare that they have no known competing financial interests or personal relationships that could have appeared to influence the work reported in this paper.

Data availability

Data will be made available on request.

Acknowledgement

We acknowledge financial support by internal funding from the University of Hong Kong and by the General Research Grant Council of Hong Kong (GRF #17306419) to SAC and CN. We are thankful to Hamsun HS Chan for his assistance in the field and experiments.

Funding sources

This study support by internal funding from the University of Hong Kong and by the General Research Grant Council of Hong Kong (GRF #17306419) to SAC and CN.

References

Apprill, A., McNally, S., Parsons, R., Weber, L., 2015. Minor revision to V4 region SSU rRNA 806R gene primer greatly increases detection of SAR11 bacterioplankton. Aquat. Microb. Ecol. 75.
Archana, A., Thibodeau, B., Geeraert, N., Xu, M.N., Kao, S.-J., Baker, D.M., 2018. Nitrogen sources and cycling revealed by dual isotopes of nitrate in a complex urbanized environment. Water Res. 142, 459–470.
Baik, K.S., Park, Y.-D., Seong, C.N., Kim, E.M., Bae, K.S., Chun, J., 2006. Glaciecola nitratireducens sp. nov., isolated from seawater. Int. J. Syst. Evol. Microbiol. 56 (9), 2185–2188.
Bertagnolli, A.D., Stewart, F.J., 2018. Microbial niches in marine oxygen minimum zones. Nat. Rev. Microbiol. 16 (12), 723–729.
Bittig, H.C., Körtzinger, A., Neill, C., van Ooijen, E., Plant, J.N., Hahn, J., Johnson, K.S., Yang, B., Emerson, S.R., 2018. Oxygen optode sensors: principle, characterization, calibration, and application in the ocean. Front. Mar. Sci. 4 (429).
Bowman, J., 2014. The Family Cryomorphaceae. The Prokaryotes: Other Major Lineages of Bacteria and The Archaea, pp. 539–550.
Bowman, J.P., McCammon, S.A., Brown, J.L., McMeekin, T.A., 1998. Glaciecola punicea gen. nov., sp. nov. and Glaciecola pallidula gen. nov., sp. nov.: psychrophilic bacteria from Antarctic sea-ice habitats. Int. J. Syst. Evol. Microbiol. 48 (4), 1213–1222.
Breitburg, D., Levin, L.A., Oschlies, A., Grégoire, M., Chavez, F.P., Conley, D.J., Garçon, V., Gilbert, D., Gutiérrez, D., Isensee, K., Jacinto, G.S., Limburg, K.E., Montes, I., Naqvi, S.W.A., Pitcher, G.C., Rabalais, N.N., Roman, M.R., Rose, K.A., Seibel, B.A., Telszewski, M., Yasuhara, M., Zhang, J., 2018. Declining oxygen in the global ocean and coastal waters. Science 359 (6371), eaam7240.
Brown, M.V., Lauro, F.M., DeMaere, M.Z., Muir, L., Wilkins, D., Thomas, T., Riddle, M.J., Fuhrman, J.A., Andrews-Pfannkoch, C., Hoffman, J.M., McQuaid, J.B., Allen, A., Rintoul, S.R., Cavicchioli, R., 2012. Global biogeography of SAR11 marine bacteria. Mol. Syst. Biol. 8 (1), 595.
Bueno, E., Mesa, S., Bedmar, E.J., Richardson, D.J., Delgado, M.J., 2011. Bacterial adaptation of respiration from oxic to microoxic and anoxic conditions: redox control. Antioxid. Redox Signal. 16 (8), 819–852.
Button, D.K., 1998. Nutrient uptake by microorganisms according to kinetic parameters from theory as related to cytoarchitecture. Microbiol. Mol. Biol. Rev. 62 (3), 636–645.
Calvert, S.E., Price, N.B., 1971. Upwelling and nutrient regeneration in the Benguela Current, October, 1968. Deep-Sea Res. Oceanogr. Abstr. 18 (5), 505–523.
Canfield, D.E., Kristensen, E., Thamdrup, B., 2005. Aquatic Geomicrobiology.
Canfield, D.E., Kraft, B., Löscher, C.R., Boyle, R.A., Thamdrup, B., Stewart, F.J., 2019. The regulation of oxygen to low concentrations in marine oxygen-minimum zones. J. Mar. Res. 77 (3), 297–324.
Caporaso, J.G., Lauber, C.L., Walters, W.A., Berg-Lyons, D., Lozupone, C.A., Turnbaugh, P.J., Fierer, N., Knight, R., 2011. Global patterns of 16S rRNA diversity

at a depth of millions of sequences per sample. Proc. Natl. Acad. Sci. 108 (Supplement 1), 4516–4522.
Carlson, C.A., Morris, R., Parsons, R., Treusch, A.H., Giovannoni, S.J., Vergin, K., 2009. Seasonal dynamics of SAR11 populations in the euphotic and mesopelagic zones of the northwestern Sargasso Sea. ISME J. 3 (3), 283–295.
Chen, Z., Wang, B., Xu, C., Zhang, Z., Li, S., Hu, J., 2022. Interannual variabilities, long-term trends, and regulating factors of low-oxygen conditions in the coastal waters off Hong Kong. Biogeosciences 19 (14), 3469–3490.
Chu, X., Wang, X., Cheung, L.S., Feng, X., Ang, P., Lee, S.Y., Crowe, S.A., Luo, H., 2022. Coastal transient niches shape the microdiversity pattern of a bacterioplankton population with reduced genomes. mBio 13 (4), e00571-00522.
Cottrell, M.T., Kirchman, D.L., 2000. Community composition of marine bacterioplankton determined by 16S rRNA gene clone libraries and fluorescence in situ hybridization. Appl. Environ. Microbiol. 66 (12), 5116–5122.
Delgado-Baquerizo, M., Giaramida, L., Reich, P.B., Khachane, A.N., Hamonts, K., Edwards, C., Lawton, L.A., Singh, B.K., 2016. Lack of functional redundancy in the relationship between microbial diversity and ecosystem functioning. J. Ecol. 104 (4), 936–946.
Diaz, R.J., Rosenberg, R., 2008. Spreading dead zones and consequences for marine ecosystems. Science 321 (5891), 926–929.
Dupont, C.L., Larsson, J., Yooseph, S., Ininbergs, K., Goll, J., Asplund-Samuelsson, J., McCrow, J.P., Celepli, N., Allen, L.Z., Ekman, M., Lucas, A.J., Hagström, Å., Thiagarajan, M., Brindefalk, B., Richter, A.R., Andersson, A.F., Tenney, A., Lundin, D., Tovchigrechko, A., Nylander, J.A.A., Brami, D., Badger, J.H., Allen, A.E., Rusch, D.B., Hoffman, J., Norrby, E., Friedman, R., Pinhassi, J., Venter, J.C., Bergman, B., 2014. Functional Tradeoffs Underpin Salinity-Driven Divergence in Microbial Community Composition. PLOS ONE 9 (2), e89549.
Dupont, C.L., Rusch, D.B., Yooseph, S., Lombardo, M.-J., Alexander Richter, R., Valas, R., Novotny, M., Yee-Greenbaum, J., Selengut, J.D., Haft, D.H., Halpern, A.L., Lasken, R. S., Nealson, K., Friedman, R., Craig Venter, J., 2012. Genomic insights to SAR86, an abundant and uncultivated marine bacterial lineage. ISME J. 6 (6), 1186–1199.
Durham, B.P., Grote, J., Whittaker, K.A., Bender, S.J., Luo, H., Grim, S.L., Brown, J.M., Casey, J.R., Dron, A., Florez-Leiva, L., Krupke, A., Luria, C.M., Mine, A.H., Nigro, O. D., Pather, S., Talarmin, A., Wear, E.K., Weber, T.S., Wilson, J.M., Church, M.J., DeLong, E.F., Karl, D.M., Steward, G.F., Eppley, J.M., Kyrpides, N.C., Schuster, S., Rappé, M.S., 2014. Draft genome sequence of marine alphaproteobacterial strain HIMB11, the first cultivated representative of a unique lineage within the Roseobacter clade possessing an unusually small genome. Stand. Genomic Sci. 9 (3), 632–645.
Edgar, R.C., Haas, B.J., Clemente, J.C., Quince, C., Knight, R., 2011. UCHIME improves sensitivity and speed of chimera detection. Bioinformatics 27 (16), 2194–2200.
Environmental Protection Department, 2019. Marine Water Quality in Hong Kong in 2019. Environmental Protection Department, T.G.o.t.H.K.S.A.R., Hong Kong.
Environmental Protection Department, 2020. Marine Water Quality in Hong Kong in 2020. Environmental Protection Department, T.G.o.t.H.K.S.A.R., Hong Kong.
Environmental Protection Department, 2021. Marine Water Quality in Hong Kong in 2021. Environmental Protection Department, T.G.o.t.H.K.S.A.R., Hong Kong.
Fuenzalida, R., Schneider, W., Garcés-Vargas, J., Bravo, L., Lange, C., 2009. Vertical and horizontal extension of the oxygen minimum zone in the eastern South Pacific Ocean. Deep Sea Res. Part II Topical Stud. Oceanogr. 56 (16), 992–1003.
García-Robledo, E., Corzo, A., Papaspyrou, S., 2014. A fast and direct spectrophotometric method for the sequential determination of nitrate and nitrite at low concentrations in small volumes. Mar. Chem. 162, 30–36.
Garcia-Robledo, E., Borisov, S., Klimant, I., Revsbech, N.P., 2016. Determination of respiration rates in water with sub-micromolar oxygen concentrations. Front. Mar. Sci. 3.
del Giorgio, P.A., Duarte, C.M., 2002. Respiration in the open ocean. Nature 420 (6914), 379–384.
Gong, G.-C., Shiah, F.-K., Liu, K.-K., Wen, Y.-H., Ming-Hsin, L., 2000. Spatial and temporal variation of chlorophyll a, primary productivity and chemical hydrography in the southern East China Sea. Cont. Shelf Res. 20 (4), 411–436.
Gong, X., Garcia-Robledo, E., Schramm, A., Revsbech, N.P., 2016. Respiratory kinetics of marine bacteria exposed to decreasing oxygen concentrations. Appl. Environ. Microbiol. 82 (5), 1412–1422.
Gram, L., Melchiorsen, J., Bruhn, J.B., 2010. Antibacterial Activity of Marine Culturable Bacteria Collected from a Global Sampling of Ocean Surface Waters and Surface Swabs of Marine Organisms. Mar. Biotechnol. 12 (4), 439–451.
Grasshoff, K., Kremling, K., Ehrhardt, M., 2009. Methods of Seawater Analysis, Third, Completely Revised and Extended edition. Wiley.
Han, P., Li, Y., Yang, X., Xue, L., Zhang, L., 2017. Effects of aerobic respiration and nitrification on dissolved inorganic nitrogen and carbon dioxide in human-perturbed eastern Jiaozhou Bay, China. Mar. Pollut. Bull. 124 (1), 449–458.
Hawley, A.K., Torres-Beltrán, M., Zaikova, E., Walsh, D.A., Mueller, A., Scofield, M., Kheirandish, S., Payne, C., Pakhomova, L., Bhatia, M., Shevchuk, O., Gies, E.A., Fairley, D., Malfatti, S.A., Norbeck, A.D., Brewer, H.M., Pasa-Tolic, L., del Rio, T.G., Suttle, C.A., Tringe, S., Hallam, S.J., 2017. A compendium of multi-omic sequence information from the Saanich Inlet water column. Scientific Data 4 (1), 170160.
Holtappels, M., Tiano, L., Kalvelage, T., Lavik, G., Revsbech, N.P., Kuypers, M.M.M., 2014. Aquatic respiration rate measurements at low oxygen concentrations. PLoS One 9 (2), e89369.
Hsiao, S.S.Y., Hsu, T.C., Liu, J.w., Xie, X., Zhang, Y., Lin, J., Wang, H., Yang, J.Y.T., Hsu, S.C., Dai, M., Kao, S.J., 2014. Nitrification and its oxygen consumption along the turbid Chang Jiang River plume. Biogeosciences 11 (7), 2083–2098.
Iriarte, A., de Madariaga, I., Diez-Garagarza, F., Revilla, M., Orive, E., 1997. Primary plankton production, respiration and nitrification in a shallow temperate estuary during summer. J. Exp. Mar. Biol. Ecol. 208 (1), 127–151.
James, A.K., Passow, U., Brzezinski, M.A., Parsons, R.J., Trapani, J.N., Carlson, C.A., 2017. Elevated pCO2 enhances bacterioplankton removal of organic carbon. PLOS ONE 12 (3), e0173145.
Jensen, L., Sand-jensen, K., Marcher, S., Hansen, M., 1990. Plankton community respiration along a nutrient gradient in a shallow Danish estuary. Mar. Ecol. Progr. Ser. 61, 75–85.
Jing, H., Xia, X., Suzuki, K., Liu, H., 2013. Vertical profiles of bacteria in the tropical and subarctic oceans revealed by pyrosequencing. PLoS One 8 (11), e79423.
Johnson, M.J., 1967. Aerobic microbial growth at low oxygen concentrations. J. Bacteriol. 94 (1), 101–108.
Kalvelage, T., Lavik, G., Jensen, M.M., Revsbech, N.P., Löscher, C., Schunck, H., Desai, D. K., Hauss, H., Kiko, R., Holtappels, M., LaRoche, J., Schmitz, R.A., Graco, M.I., Kuypers, M.M.M., 2015. Aerobic microbial respiration in oceanic oxygen minimum zones. PLoS One 10 (7), e0133526.
Keeling, R., Arne, K., Gruber, N., 2010. Ocean deoxygenation in a warming world. Annu. Rev. Mar. Sci. 2, 199–229.
Khachikyan, A., Milucka, J., Littmann, S., Ahmerkamp, S., Meador, T., Könneke, M., Burg, T., Kuypers, M.M.M., 2019. Direct cell mass measurements expand the role of small microorganisms in nature. Appl. Environ. Microbiol. 85 (14), e00493-00419.
Leong, L.S., Tanner, P.A., 1999. Comparison of methods for determination of organic carbon in marine sediment. Mar. Pollut. Bull. 38 (10), 875–879.
Lønborg, C., Müller, M., Butler, E.C.V., Jiang, S., Ooi, S.K., Trinh, D.H., Wong, P.Y., Ali, S. M., Cui, C., Siong, W.B., Yando, E.S., Friess, D.A., Rosentreter, J.A., Eyre, B.D., Martin, P., 2021. Nutrient cycling in tropical and temperate coastal waters: Is latitude making a difference? Estuar. Coast. Shelf Sci. 262, 107571.
López-Pérez, M., Haro-Moreno, J.M., Iranzo, J., Rodriguez-Valera, F., Bowman, J., 2020. Genomes of the candidatus actinomarinales order: highly streamlined marine epipelagic actinobacteria. mSystems 5 (6), e01041-01020.
Lorenzen, C.J., 1967. Determination of chlorophyll and pheo-pigments: spectrophotometric equations. Limnol. Oceanogr. 12 (2), 343–346.
Luo, H., Moran, M.A., 2014. Evolutionary ecology of the marine roseobacter clade. Microbiol. Mol. Biol. Rev. 78 (4), 573–587.
Martinez-Malaxetxebarria, I., Muts, R., van Dijk, L., Parker, C.T., Miller, W.G., Huynh, S., Gaastra, W., van Putten, J.P., Fernandez-Astorga, A., Wösten, M.M., 2012. Regulation of energy metabolism by the extracytoplasmic function (ECF) σ factors of Arcobacter butzleri. PLoS One 7 (9), e44796.
Medina-Sánchez, J., Herrera, G., Durán Romero, C., Villar-Argaiz, M., Carrillo, P., 2017. Optode use to evaluate microbial planktonic respiration in oligotrophic ecosystems as an indicator of environmental stress. Aquat. Sci. 79.
Michiels, C.C., Huggins, J.A., Giesbrecht, K.E., Spence, J.S., Simister, R.L., Varela, D.E., Hallam, S.J., Crowe, S.A., 2019. Rates and pathways of N2 production in a persistently Anoxic Fjord: Saanich Inlet, British Columbia. Front. Mar. Sci. 6.
Miller, W.G., Parker, C.T., Rubenfield, M., Mendz, G.L., Wösten, M.M., Ussery, D.W., Stolz, J.F., Binnewies, T.T., Hallin, P.F., Wang, G., Malek, J.A., Rogosin, A., Stanker, L.H., Mandrell, R.E., 2007. The complete genome sequence and analysis of the epsilonproteobacterium Arcobacter butzleri. PLoS One 2 (12), e1358.
Morris, R.L., Schmidt, T.M., 2013. Shallow breathing: bacterial life at low O2. Nat. Rev. Microbiol. 11 (3), 205–212.
Munson-McGee, J.H., Lindsay, M.R., Sintes, E., Brown, J.M., D'Angelo, T., Brown, J., Lubelczyk, L.C., Tomko, P., Emerson, D., Orcutt, B.N., Poulton, N.J., Herndl, G.J., Stepanauskas, R., 2022. Decoupling of respiration rates and abundance in marine prokaryoplankton. Nature 612 (7941), 764–770.
Murillo, A.A., Ramírez-Flandes, S., DeLong, E.F., Ulloa, O., 2014. Enhanced metabolic versatility of planktonic sulfur-oxidizing γ-proteobacteria in an oxygen-deficient coastal ecosystem. Front. Mar. Sci. 1 (18).
Ngugi, D.K., Stingl, U., 2018. High-quality draft single-cell genome sequence of the NS5 marine group from the coastal red sea. Genome Announc 6 (25), e00565-00518.
Oschlies, A., Brandt, P., Stramma, L., Schmidtko, S., 2018. Drivers and mechanisms of ocean deoxygenation. Nat. Geosci. 11 (7), 467–473.
Qian, W., Gan, J., Liu, J., He, B., Lu, Z., Guo, X., Wang, D., Guo, L., Huang, T., Dai, M., 2018. Current status of emerging hypoxia in a eutrophic estuary: the lower reach of the Pearl River Estuary, China. Estuar. Coast. Shelf Sci. 205, 58–67.
Rabalais, N.N., Turner, R.E., Dortch, Q., Justic, D., Bierman, V.J., Wiseman, W.J., 2002. Nutrient-enhanced productivity in the northern Gulf of Mexico: past, present and future. Hydrobiologia 475 (1), 39–63.
Raven, J.A., Geider, R.J., 1988. Temperature and algal growth. New Phytol. 110 (4), 441–461.
Revsbech, N.P., Glud, R.N., 2009. Biosensor for laboratory and lander-based analysis of benthic nitrate plus nitrite distribution in marine environments. Limnol. Oceanogr. Methods 7 (11), 761–770.
Rice, C.W., Hempfling, W.P., 1978. Oxygen-limited continuous culture and respiratory energy conservation in Escherichia coli. J. Bacteriol. 134 (1), 115–124.
Roalkvam, I., Drønen, K., Stokke, R., Daae, F.L., Dahle, H., Steen, I.H., 2015. Physiological and genomic characterization of Arcobacter anaerophilus IR-1 reveals new metabolic features in epsilonproteobacteria. Front. Microbiol. 6, 987.
Robinson, C., 2019. Microbial respiration, the engine of ocean deoxygenation. Front. Mar. Sci. 5 (533).
Robinson, C., Williams, P., 2005. Respiration and its measurements in surface marine waters. Resp. Aquat. Syst. 147–180.
Robinson, C., Serret, P., Tilstone, G., Teira, E., Zubkov, M.V., Rees, A.P., Woodward, E.M. S., 2002. Plankton respiration in the Eastern Atlantic Ocean. Deep-Sea Res. I Oceanogr. Res. Pap. 49 (5), 787–813.
Schloss, P.D., Gevers, D., Westcott, S.L., 2011. Reducing the effects of PCR amplification and sequencing artifacts on 16S rRNA-based studies. PLoS One 6 (12), e27310.
Schloss, P.D., Westcott, S.L., Ryabin, T., Hall, J.R., Hartmann, M., Hollister, E.B., Lesniewski, R.A., Oakley, B.B., Parks, D.H., Robinson, C.J., Sahl, J.W., Stres, B.,

Thallinger, G.G., Horn, D.J.V., Weber, C.F., 2009. Introducing mothur: Open-Source, Platform-Independent, Community-Supported Software for Describing and Comparing Microbial Communities. Appl. Environ. Microbiol. 75 (23), 7537–7541.
Schmidtko, S., Stramma, L., Visbeck, M., 2017. Decline in global oceanic oxygen content during the past five decades. Nature 542 (7641), 335–339.
Seibert, E., Tracy, T.S., 2021. Fundamentals of enzyme kinetics: michaelis-menten and non-michaelis-type (atypical) enzyme kinetics. Methods Mol. Biol. 2342, 3–27.
Sinkko, H., Hepolehto, I., Lyra, C., Rinta-Kanto, J.M., Villnäs, A., Norkko, J., Norkko, A., Timonen, S., 2019. Increasing oxygen deficiency changes rare and moderately abundant bacterial communities in coastal soft sediments. Sci. Rep. 9 (1), 16341.
van der Stel, A.-X., Wösten, M.M.S.M., 2019. Regulation of respiratory pathways in campylobacterota: a review. Front. Microbiol. 10, 1719.
Stevens, H., Ulloa, O., 2008. Bacterial diversity in the oxygen minimum zone of the eastern tropical South Pacific. Environ. Microbiol. 10 (5), 1244–1259.
Stolper, D.A., Revsbech, N.P., Canfield, D.E., 2010. Aerobic growth at nanomolar oxygen concentrations. Proc. Natl. Acad. Sci. 107 (44), 18755–18760.
Stramma, L., Schmidtko, S., Levin, L.A., Johnson, G.C., 2010. Ocean oxygen minima expansions and their biological impacts. Deep-Sea Res. I Oceanogr. Res. Pap. 57 (4), 587–595.
Stramma, L., Oschlies, A., Schmidtko, S., 2012. Mismatch between observed and modeled trends in dissolved upper-ocean oxygen over the last 50 yr. Biogeosciences 9 (10), 4045–4057.
Tiano, L., Garcia-Robledo, E., Dalsgaard, T., Devol, A.H., Ward, B.B., Ulloa, O., Canfield, D.E., Peter Revsbech, N., 2014a. Oxygen distribution and aerobic respiration in the north and south eastern tropical Pacific oxygen minimum zones. Deep-Sea Res. I Oceanogr. Res. Pap. 94, 173–183.
Tiano, L., Garcia-Robledo, E., Revsbech, N.P., 2014b. A new highly sensitive method to assess respiration rates and kinetics of natural planktonic communities by use of the switchable trace oxygen sensor and reduced oxygen concentrations. PLoS One 9 (8), e105399.
Torres-Beltrán, M., Mueller, A., Scofield, M., Pachiadaki, M.G., Taylor, C., Tyshchenko, K., Michiels, C., Lam, P., Ulloa, O., Jürgens, K., Hyun, J.-H., Edgcomb, V.P., Crowe, S.A., Hallam, S.J., 2019. Sampling and processing methods impact microbial community structure and potential activity in a seasonally Anoxic Fjord: Saanich Inlet, British Columbia. Front. Mar. Sci. 6.
Traving, S.J., Bentzon-Tilia, M., Knudsen-Leerbeck, H., Mantikci, M., Hansen, J.L.S., Stedmon, C.A., Sørensen, H., Markager, S., Riemann, L., 2016. Coupling bacterioplankton populations and environment to community function in coastal temperate waters. Front. Microbiol. 7.
Trojan, D., Garcia-Robledo, E., Meier, D.V., Hausmann, B., Revsbech, N.P., Eichorst, S.A., Woebken, D., Bernstein, H.C., 2021. Microaerobic lifestyle at nanomolar O₂ concentrations mediated by low-affinity terminal oxidases in abundant soil bacteria. mSystems 6 (4), e00250-00221.
Tsementzi, D., Wu, J., Deutsch, S., Nath, S., Rodriguez-R, L.M., Burns, A.S., Ranjan, P., Sarode, N., Malmstrom, R.R., Padilla, C.C., Stone, B.K., Bristow, L.A., Larsen, M., Glass, J.B., Thamdrup, B., Woyke, T., Konstantinidis, K.T., Stewart, F.J., 2016. SAR11 bacteria linked to ocean anoxia and nitrogen loss. Nature 536 (7615), 179–183.
Vikström, K., Tengberg, A., Wikner, J., 2019. Improved accuracy of optode-based oxygen consumption measurements by removal of system drift and nonlinear derivation. Limnol. Oceanogr. Methods 17 (3), 179–189.
Wallenstein, M., Allison, S.D., Ernakovich, J., Steinweg, J.M., Sinsabaugh, R., 2011. Controls on the temperature sensitivity of soil enzymes: a key driver of in situ enzyme activity rates. Soil Enzymol. 245–258.
Wang, K., Kitney, R.I., Seakins, J.W., Hjelm, M., 1992. Study of the relationship between estimates of enzyme kinetic parameters. J. Theor. Biol. 155 (4), 485–495.
Ward, B.B., 2008. Nitrification in Marine Systems. Nitrogen in the Marine Environment, 2, pp. 199–261.
Westcott, S.L., Schloss, P.D., 2017. OptiClust, an Improved Method for Assigning Amplicon-Based Sequence Data to Operational Taxonomic Units. mSphere 2 (2), e00073-00017.
Wikner, J., Vikström, K., Verma, A., 2023. Regulation of marine plankton respiration: a test of models. Front. Mar. Sci. 10.
Wright, J.J., Konwar, K.M., Hallam, S.J., 2012. Microbial ecology of expanding oxygen minimum zones. Nat. Rev. Microbiol. 10 (6), 381–394.
Wyrtki, K., 1962. The oxygen minima in relation to ocean circulation. Deep-Sea Res. Oceanogr. Abstr. 9 (1), 11–23.
Yau, Y.Y., Baker, D.M., Thibodeau, B., 2020. Quantifying the impact of anthropogenic atmospheric nitrogen deposition on the generation of hypoxia under future emission scenarios in chinese coastal waters. Environ. Sci. Technol. 54 (7), 3920–3928.
Yuan, X., Yin, K.D., Harrison, P., Cai, W.-J., He, L., Xu, J., 2010. Bacterial production and respiration in subtropical Hong Kong waters: Influence of the Pearl River discharge and sewage effluent. Aquat. Microb. Ecol. 58.
Zaikova, E., Walsh, D.A., Stilwell, C.P., Mohn, W.W., Tortell, P.D., Hallam, S.J., 2010. Microbial community dynamics in a seasonally anoxic fjord: Saanich Inlet, British Columbia. Environ. Microbiol. 12 (1), 172–191.
Zhang, R., Liu, B., Lau, S.C.K., Ki, J.-S., Qian, P.-Y., 2007. Particle-attached and free-living bacterial communities in a contrasting marine environment: Victoria Harbor, Hong Kong. FEMS Microbiol. Ecol. 61 (3), 496–508.